

PREDICTING FATIGUE DURING ELECTRICALLY STIMULATED NON-ISOMETRIC CONTRACTIONS

M. SUSAN MARION, PhD,¹ ANTHONY S. WEXLER, PhD,^{1,2} and MAURY L. HULL, PhD^{1,2}

¹ Biomedical Engineering Program, Bainer Hall, University of California, One Shields Avenue, Davis, California 95616, USA

² Mechanical and Aerospace Engineering, University of California, Davis, California, USA

Accepted 20 October 2009

ABSTRACT: Mathematical prediction of power loss during electrically stimulated contractions is of value to those trying to minimize fatigue and to those trying to decipher the relative contributions of force and velocity. Our objectives were to: (1) develop a model of non-isometric fatigue for electrical stimulation-induced, open-chain, repeated extensions of the leg at the knee; and (2) experimentally validate the model. A computer-controlled stimulator sent electrical pulses to surface electrodes on the thighs of 17 able-bodied subjects. Isometric and non-isometric non-fatiguing and fatiguing leg extension torque and/or angle at the knee were measured. Two existing mathematical models, one of non-isometric force and the other of isometric fatigue, were combined to develop the non-isometric force-fatigue model. Angular velocity and 3 new parameters were added to the isometric fatigue model. The new parameters are functions of parameters within the force model, and therefore additional measurements from the subject are not needed. More than 60% of the variability in the measurements was explained by the new force-fatigue model. This model can help scientists investigate the etiology of non-isometric fatigue and help engineers to improve the task performance of functional electrical stimulation systems.

Muscle Nerve 41: 857–867, 2010

Functional electrical stimulation (FES) may be used by individuals with paralysis due to either stroke or spinal cord injury (SCI) to regain functional movement. Mathematical simulations can be used to identify stimulation strategies that produce desired forces and motions, but these simulations must account for muscle fatigue. Otherwise, the duration of the task will limit the predictive ability of the model.

During non-isometric contractions, muscle fatigue is exhibited as a reduction in muscle power.¹ Power is determined by the number and force of the strongly bound cross-bridges and the rate of cross-bridge cycling within the muscle.¹ In an effort to determine the relative contribution of these factors to loss of power, the relative loss of muscle isometric force, non-isometric force, and velocity are often compared during and/or following fatiguing contractions.^{2–5} Because the cause of fatigue is multifactorial and task-dependent, there is no single approach to the study of fatigue.⁶ Therefore, relationships between loss of power, ve-

locity, force, and the dynamics of the cross-bridge cycle have been difficult to define quantitatively. A mathematical model capable of predicting muscle power, velocity, force, and fatigue could be used to derive specific relationships between tasks and their associated losses of power, force, and velocity. In addition, a validated model could predict force during fatiguing contractions in testing situations where force cannot be measured easily, such as during general non-isometric leg extensions.

Models of non-isometric, non-fatiguing contractions^{7–9} and models of isometric fatiguing contractions^{10–15} have been developed, yet an experimentally validated model that can predict force and motion before and during fatiguing non-isometric contractions in humans has not appeared in the literature. Xia and Law¹⁶ developed a model that has the potential to predict non-isometric fatigue during physiological stimulation. Unfortunately, predictions were not verified experimentally. Without experimental validation under different testing conditions, the accuracy and generalizability of the model are unknown, and the model may not predict FES-induced fatigue because recruitment during electrical stimulation is non-physiological. Likewise, a simple dynamic muscle fatigue model that does not include limb dynamics was developed by Ma and colleagues,¹⁷ but it was not experimentally validated.

The non-isometric force model by Perumal and colleagues^{8,9} and the isometric fatigue model by Ding and colleagues^{11,18} and Marion and colleagues¹⁹ have been experimentally validated in humans to predict such force and fatigue in response to a wide range of clinically relevant electrical stimulation patterns. If the non-isometric force model could be integrated with a non-isometric fatigue model, then power could be predicted before and during non-isometric fatiguing contractions. As compared with the biomechanics of a leg attached to an exercise dynamometer, the kinetics and kinematics of a general non-isometric leg extension more closely resemble the leg biomechanics during natural movement during a gait cycle. For this reason, and because the non-isometric force model⁸ can predict the forces during general non-isometric leg extensions, we chose general non-isometric leg extensions to develop our model of non-isometric muscle fatigue. The term leg is defined as that section of the lower limb between

Abbreviations: ANOVA, analysis of variance; CFT, constant frequency train; FES, functional electrical stimulation; ITT, interpolated twitch tension; MVIC, maximal voluntary isometric contraction; SCI, spinal cord injury; TTI, torque time interval; VFT, variable frequency train

Key words: functional electrical stimulation (FES); mathematical model; muscle fatigue; non-isometric

Correspondence to: M.S. Marion; e-mail: msmarion@ucdavis.edu

© 2010 Wiley Periodicals, Inc.
Published online 12 March 2010 in Wiley InterScience (www.interscience.wiley.com). DOI 10.1002/mus.21603

the knee and ankle. The phrase general non-isometric indicates that the leg is not attached to the exercise dynamometer. It is free to move at any velocity in more than one plane. The objectives of this study were to: (1) develop a model of non-isometric fatigue for electrical stimulation-induced, open-chain, repeated extensions of the leg at the knee; and (2) experimentally validate the model.

METHODS

Mathematical Model. The force-fatigue model developed by Ding and colleagues^{8,9,11,18} was used for this study (see Table 1 for definitions of symbols). The force model describes muscle activation, contraction dynamics, the force-angle relationship, and the force-angular velocity relationship. The input is the time the pulses are delivered, and the output is the force at the ankle predicted for each time-point:

$$\frac{dC_N}{dt} = \frac{1}{\tau_c} \sum_{i=1}^n R_i \exp\left(-\frac{t-t_i}{\tau_c}\right) - \frac{C_N}{\tau_c} \quad (1)$$

$$R_i = \begin{cases} 1 & i = 1 \\ 1 + (R_0 - 1) \exp\left(-\frac{t_i - t_{i-1}}{\tau_c}\right) & i > 1 \end{cases} \quad (1a)$$

$$\frac{dF}{dt} = [G + A] \frac{C_N}{K_m + C_N} - \frac{F}{\tau_1 + \tau_2} \frac{C_N}{K_m + C_N} \quad (2)$$

$$A = A_{90}(a(90 - \theta)^2 + b(90 - \theta) + 1) \quad (2a)$$

$$G = V_1 \theta \exp(-V_2 \theta) \frac{d\theta}{dt} \quad (2b)$$

$$\frac{d^2\theta}{dt^2} = \frac{L}{I} [(F_{load} + F_M) \cos(\theta + \lambda) - F] \quad (3)$$

Equation (1) models the rate-limiting step that leads to the formation of strongly bound cross-bridges, and it represents the activation dynamics. Equation (2) describes the generation of the muscle force component of torque. It was derived from a Maxwell model of linear viscoelasticity in series with a motor.¹⁸ The terms A and G represent the torque-angle²⁰ and torque-angular velocity⁹ relationships, respectively. The Michaelis-Menten term, $C_N/(K_m + C_N)$, scaled by A and G , drives the development of force. The last term in eq. (2) accounts for the force decay over two time constants, τ_1 and τ_2 . Equation (3) models the dynamics of the leg distal to the knee. The term F_M represents the resistance to knee extension due to the weight of the leg and all other passive resistance about the knee joint, whereas F_{load} is the load applied at the ankle (0–9.08 kg).

The fatigue model monitors changes in the three force model parameters that change with fatigue, A_{90} , K_m , and τ_1 . The input is instantaneous force from the force model (once all force and fatigue model parameters have been identified), and the output is A_{90} , K_m , and τ_1 :

$$\frac{dA_{90}}{dt} = -\frac{A_{90} - A_{90,0}}{\tau_{fat}} + \left(\alpha_A + \beta_A \frac{d\theta}{dt}\right) F \quad (4)$$

$$K_m = K_{m1} + K_{m2} \quad (5)$$

$$\frac{dK_{m1}}{dt} = -\frac{K_{m1} - K_{m1,0}}{\tau_{fat}} + \left(\alpha_{K_m} + \beta_{K_m} \frac{d\theta}{dt}\right) F \quad (6)$$

$$\frac{dK_{m2}}{dt} = -\left(\alpha_{K_m} + \beta_{K_m} \frac{d\theta}{dt}\right) F \quad (7)$$

$$\frac{d\tau_1}{dt} = -\frac{\tau_1 - \tau_{1,0}}{\tau_{fat}} + \left(\alpha_{\tau_1} + \beta_{\tau_1} \frac{d\theta}{dt}\right) F \quad (8)$$

The time constant, τ_{fat} , characterizes the rate of change of parameters, A_{90} , τ_1 , and K_m , from the pre-fatigue values ($A_{90,0}$, $\tau_{1,0}$, and $K_{m,0}$) to steady state. All of the isometric terms (those without $d\theta/dt$) have been reported previously,^{11,19} and the same procedures were used here to identify the isometric values.

Because the relationship between force and velocity has been shown to change with fatigue,^{2,5} the $\beta d\theta/dt$ terms were added to the equations. Preliminary data collection and analyses indicated that this was likely to be a successful approach.

Experimental Procedures. Seventeen healthy subjects, 8 men and 9 women (ages 19–26 years), with no history of lower extremity orthopedic problems, voluntarily participated in this study and signed informed consent agreements. This study was approved by the University of California Human Subjects Review Board.

The experimental setup was similar to that described previously.^{8,9,21} Briefly, subjects were seated in a backward-inclined (15° from vertical) chair of a computer-controlled dynamometer (System 2; Biodex Medical Systems, Inc., Shirley, New York). The trunk, hips, and thigh were strapped to the chair, thus fixing the hip angle and limiting leg movement. The ankle was strapped to the lever arm of the dynamometer for the isometric and iso-velocity tests. The axis of rotation of the knee joint was aligned with the axis of rotation of the dynamometer. A custom-built electrogoniometer was strapped to the lower limb and trunk to measure the knee angle. Customized software (LabView 8.0, National Instruments Corp., Austin, Texas) collected the digitized voltage signals at 300 Hz from the dynamometer torque transducer and the electrogoniometer. Two 7.5 × 12.5-cm self-adhesive stimulating electrodes were placed on the skin of the right thigh, one at the proximal and the other at the distal end of the quadriceps muscles. The final electrode position was determined by the torque-time curves (which resemble the product of a forward and reverse logistic curve) at 3 isometric knee angles, 90°, 55°, and 20°, and the amount of planar movement during general non-isometric leg

Table 1. Definitions of symbols and acronyms.

Term	Unit	Definition
A_{90}	N/ms	Scaling factor reflecting magnitude of force at 90°
a	deg ⁻²	Defines parabolic shape of ankle force-knee angle relationship
α_A	ms ⁻²	Force scaling factor in fatigue model for force model parameter A
α_{K_m}	ms ⁻¹ N ⁻¹	Force scaling factor in fatigue model for force model parameter K_m
α_{τ_1}	N ⁻¹	Force scaling factor in fatigue model for force model parameter τ_1
b	deg ⁻¹	Defines parabolic shape of ankle force-knee angle relationship
β_A	ms ⁻¹ deg ⁻¹	Angular velocity × force scaling factor in fatigue model for force model parameter A
β_{K_m}	deg ⁻¹ N ⁻¹	Angular velocity × force scaling factor in fatigue model for force model parameter K_m
β_{τ_1}	ms deg ⁻¹ N ⁻¹	Angular velocity × force scaling factor in fatigue model for force model parameter τ_1
CFT	—	Constant frequency train
C_N	—	Normalized concentration of Ca ²⁺ -troponin complex
F	N	Instantaneous force at the ankle
F_{load}	N	Load applied at ankle during general non-isometric leg extensions
F_M	N	Represents the resistance to knee extension due to the weight of the leg and all other passive resistance about the knee joint.
FTI	N-s	Force time integral
I	kg-m ²	Net mass moment of inertia of the leg plus the applied load
K_m	—	Similar to Michaelis-Menten constant; affinity of actin-strong binding site for myosin
L	m	Effective moment arm from knee joint center of rotation to resultant force vector near ankle
λ	deg	90° minus the knee flexion angle of the resting non-isometric leg
n	—	Number of stimuli in train before time t
R_0	—	Characterizes the magnitude of enhancement in C_N from the following stimuli
R_i	—	Accounts for differences in activation for each pulse relative to first pulse of train
SCI	—	Spinal cord injury
t_i	ms	Time of the i th stimulation
τ_1	ms	Time constant of force decline in the absence of strongly bound cross-bridges
τ_2	ms	Time constant of force decline due to actin-myosin friction in cross-bridges
τ_c	ms	Time constant controlling the rise and decay of C_N
τ_{fat}	ms	Time constant for force model parameters A , K_m , and τ_1 during fatigue
θ	deg	Knee flexion angle, where full extension is 0°
V_1	N/deg ²	Scaling factor in the term G
V_2	deg ⁻¹	Constant
VFT	—	Variable frequency train

extensions. The position was adjusted until the plateau of the torque–time curves produced during 1-second stimulations remained constant from the beginning to the end of steady state at each knee angle. The electrodes were repositioned if the leg visibly moved out of the sagittal plane during the non-isometric extensions. In these cases, the electrode position was again tested at the 3 isometric knee angles, and the final position was a compromise between a smooth torque–time curve with a constant plateau and planar leg movement. Customized software controlled the rate that pulses were delivered by the stimulator (Grass S48) to the electrodes. An attached stimulus isolation unit (SIU8T) isolated the electrodes from ground, providing greater safety to the subject.

Each subject participated in 4 or 6 testing sessions. Ten subjects were used for model development; the remaining 7 for model validation. Subjects were asked to refrain from strenuous exercise for 24 hours prior to each testing session. Successive sessions were separated by a minimum of 48 hours, the minimum time required by the muscles to recover and again yield the maximum torque

measured prior to fatigue. During the testing sessions, stimulation trains were applied to relaxed quadriceps femoris muscles. Just before the first session, a modified interpolated twitch technique (ITT)²² was used to determine the subject's maximal voluntary isometric contraction (MVIC). In brief, a 100-Hz, 135-V 11-pulse train was delivered to the quadriceps muscle while the subject attempted to extend the fixed leg (knee angle held at 90°). Voluntary torque was considered maximal if it did not increase by >10% when the stimulus train was added. If torque increased with stimulation by >10%, subjects rested 5 min before attempting to perform another MVIC. All subjects completed this task successfully within three attempts. For the 10 model development subjects, the stimulation amplitude was set at the voltage that extended the leg plus a 9.08-kg load to ~15° while a 1-second 50-Hz train of pulses was applied. This assured a maximum range of motion for every subject for all loads, and thus a maximum range of fatigue for model development. For the 7 model validation subjects, the stimulation amplitude was set to produce 20% MVIC with the knee at 90° in

response to a 6-pulse, 100-Hz train, during every session for the entire session, as was done in the non-fatigue studies.^{8,20}

Pre-fatigue isometric, isovelocitory, and general non-isometric (Fig. 1) torque and/or angle data,⁸ as well as fatiguing isometric torque¹¹ and general non-isometric angle data in response to electrical pulse trains, were acquired from the testing sessions. The trains were either constant (CFT) or variable (VFT) frequency trains, containing equally spaced singlet pulses or an initial doublet followed by equally spaced singlet pulses, respectively. Pulse durations were 600 μ s. At the beginning of every test the quadriceps were held isometric and stimulated with 12 14CFT (i.e., CFT with 14-Hz pulse frequency), each train on for 0.8 seconds and off for 5 seconds, to potentiate the muscle.²⁰ Pre-fatigue isovelocitory torque and angle measurements were collected first. The dynamometer, set to passive mode, moved the leg at 150°/second from \sim 110° to 4°. Measurements were collected from leg extensions performed without stimulation and from extensions performed while the quadriceps were stimulated as the leg extended from 85° to 20°. There were 4 pre-fatigue testing trains, one per leg extension, a 50CFT (50 Hz) followed by 2 12.5VFTs (12.5-Hz, 5-ms between pulses within the initial doublet) and a 50CFT, each train on for 1 second and off for 10 seconds. These 4 trains were used to identify the pre-fatigue isovelocitory model parameters. The leg was rested for 4 minutes followed by collection of the pre-fatigue isometric torque measurements. Four knee angles (15°, 40°, 65°, 90°) were tested in a different order every session, which varied from subject to subject. The 4 testing trains were applied at each knee angle. The muscles rested for 4 minutes between each angle.

After a 4-minute rest, the fatiguing stimulation protocol was applied to the thigh, one fatigue session per day. One isometric (knee at 90°) and 3 general non-isometric (Fig. 1) fatigue sessions were used for model development and validation. For the general non-isometric sessions, the leg was released from the dynamometer, allowed to swing freely, and weights were applied to the ankle at 0, 4.54, or 9.08 kg. Two additional general non-isometric fatigue sessions, with 1.82- and 6.36-kg loads, were used for model validation in 9 of the model development subjects. Fourteen pairs of testing (50CFT–12.5VFT) and 182 fatiguing [33CFT (33-Hz)] trains were applied. The trains were applied as follows: 1 pair of testing trains followed by 13 fatiguing trains, repeated 14 times. The first 2 trains, that is, the first pair of testing trains, were each followed by a 10-second rest. These 2 trains produced the isometric and the general non-isometric initial (pre-fatigue) contrac-

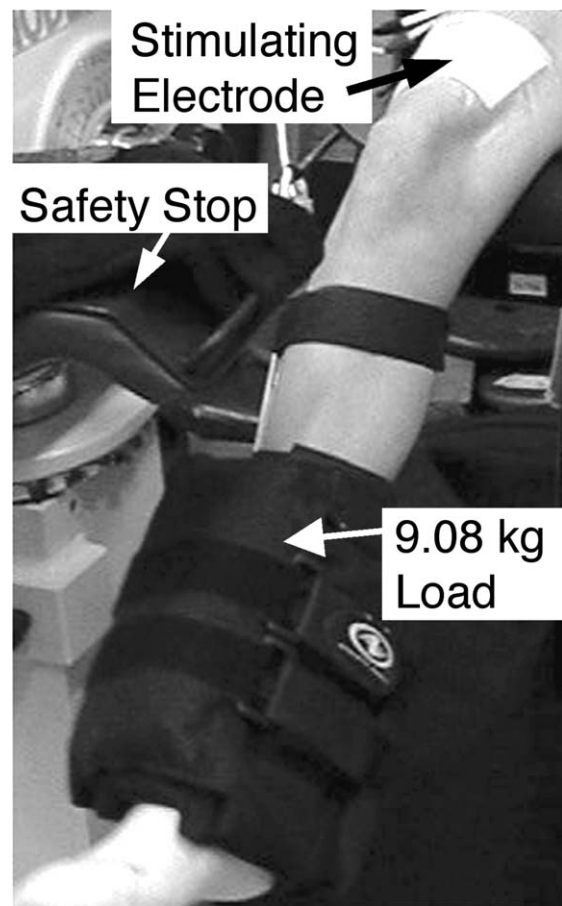


FIGURE 1. Photograph of a general non-isometric leg extension.

tions used by the model. For the isometric session, all trains were on 1 second and, after the third train, all were off 1 second.¹¹ This duty cycle is similar to that found in normal gait and has been proven effective for fatigue of the quadriceps, as well as for identification of the model parameters.¹¹ For the general non-isometric sessions the train, the off time was 1.3 seconds, the minimum time required for the leg to return to the resting position (80–90°) and for us to manually stop the oscillations with our hands. The on time was set at the time needed for the leg, with the load for that session attached, to extend to \sim 15° while the thigh was stimulated with a 50CFT. The on times varied from approximately 0.15 to 1 second, from session to session, depending on the load applied and on the subject. For the model development subjects, the on time was constant for all trains during the fatigue protocol of a given session; that is, all 210 trains had the same on time. For the model validation subjects, the number of pulses remained constant during that testing session; that is, all 210 trains delivered the same number of pulses per train.

Parameter Identification. The force–fatigue model contains a total of 19 parameters. Parameters R_0

and τ_c were held constant at 2 (unitless)¹¹ and 20 ms,²³ respectively. The remaining 17 parameters, which included A_{90} , a , b , K_m , τ_1 , τ_2 , V_1 , V_2 , L/I , and F_M from the force model, and α_A , α_{K_m} , α_{τ_1} , τ_{fat} , β_A , β_{K_m} , and β_{τ_1} from the fatigue model, required identification (see Fig. 2). Parameters A_{90} , K_m , τ_1 , τ_2 , a , b , V_1 , and V_2 were identified from the pre-fatigue isometric and isovelocity contractions from the day of the isometric fatiguing session. In addition, 13 fatigue values for parameters A_{90} , K_m , and τ_1 were identified from each 50CFT–12.5VFT pair within the isometric fatiguing protocol. Pre-fatigue values for A_{90} , K_m , and τ_1 [eq. (2)] were re-identified, and L/I and F_M [eq. (3)] were identified from the pre-fatigue general non-isometric 50CFT–12.5VFT pair on the days of the general non-isometric fatiguing sessions. Parameters β_A , β_{K_m} , and β_{τ_1} [eqs. (4)–(8)] were initially identified for the 0-, 4.54-, and 9.08-kg loads by fitting model predicted to measured angles and angular velocities from the fatiguing general non-isometric leg extensions.

Model parameters were identified through minimization of the sum-of-squares error between the measured and modeled forces (for A_{90} , K_m , τ_1 , τ_2 , V_1 , and V_2 ; from the isometric fatiguing day), between the parameter A identified from the force model and the parameter A predicted by the parabolic equation [for a and b , eq. (2a)], between the measured and modeled angles and angular velocities (for A_{90} , K_m , τ_1 , L/I , and F_M for the general non-isometric fatiguing days and for derivation of the β_A , β_{K_m} , and β_{τ_1} equations), and between the parameters A_{90} , K_m , and τ_1 derived from the force model and the parameters A_{90} , K_m , and τ_1 predicted by the fatigue model (for α_A , α_{K_m} , α_{τ_1} , and τ_{fat} ; see Fig. 2), via a particle swarm optimization algorithm.²⁴ Initially, the bounds for the candidate solutions were a factor of 10 above and below values reported previously,^{11,23,25} and then they were adjusted if necessary. A population of random guesses at the problem solution, within the bounds, was initialized. These candidate solutions were improved through an iterative process. Once a candidate “global” minimum was reached, a new population of random guesses, which included the “global” best solution, was initialized, and the iterative process was repeated. The local minimum was confirmed by using the MatLab non-linear least-squares algorithm.²⁶ The entire procedure was repeated several times to confirm that the solution had converged to the “global” minimum.

Statistical Analysis. The predictive accuracy of the model was determined by analysis of the linear regression coefficient of determination (r^2). The dependent variable was the predicted, and the in-

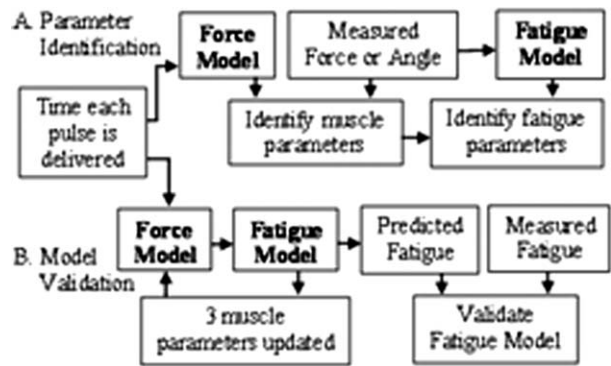


FIGURE 2. Block diagram demonstrating parameter identification (A) and prediction of fatigue (B) using the force and fatigue models. The following describes the parameter identification procedure. Muscle parameters A_{90} , K_m , τ_1 , and τ_2 [eq. (2)] were identified by fitting model-predicted forces to measured forces collected during the pre-fatigue isometric contractions on the day of the isometric fatiguing session. Parameter τ_1 was identified separately using the force at the end of each contraction. Parameter A predicted by eq. (2a) was fit to parameter A obtained from eq. (2) for all four knee angles to identify a and b . Parameters V_1 and V_2 [eq. (2)] were identified by fitting model predicted forces to measured forces collected during the isovelocity leg extensions on the day of the isometric fatiguing session. Parameters A_{90} , K_m , τ_1 [eq. (2)] were re-identified and parameters L/I and F_M [eq. (3)] were identified on the days of the general non-isometric fatiguing sessions from the pre-fatigue testing pair of contractions by fitting model-predicted knee angles to measured knee angles collected during the general non-isometric leg extensions. Parameters A_{90} , K_m , and τ_1 were also identified from the isometric fatiguing contractions. Fitting A_{90} , K_m , and τ_1 predicted by the fatigue model to A_{90} , K_m , and τ_1 obtained from the force model for the isometric pre-fatigue and isometric fatiguing contractions identified the fatigue model parameters α_A , α_{K_m} , α_{τ_1} , and τ_{fat} [eqs. (4)–(8)]. Initially, parameters β_A , β_{K_m} , and β_{τ_1} [eqs. (4)–(8)] were identified by fitting model-predicted angles and angular velocities to the measured values collected during the fatiguing general non-isometric leg extensions when the 0-, 4.5-, and 9.1-kg loads were applied. Equations for β_A , β_{K_m} , and β_{τ_1} [eqs. (4a), (7a), and (8a)] were then derived from correlations with the parameters in the force model.

dependent variable was the measured angular excursion. For this study, angular excursion is defined as the difference between the initial and final knee angles of every leg extension. The initial angle was the resting angle just prior to stimulation. The final angle was the minimum flexion angle the leg reached during each extension. For the lower loads, this minimum angle was often reached after cessation of stimulation. Both a fixed slope of unity and a y-intercept of zero were used. Ideally, if the predictive accuracy of the model was 100%, then the linear regression r^2 would be unity. The effect of load on the r^2 was determined using a one-factor repeated-measures analysis of variance (ANOVA) followed by Tukey’s post hoc tests. The independent variable was load (0, 1.82, 4.54, 6.36, and 9.08 kg, and isometric), and the dependent variable was the r^2 value.

The effect of load on the change in predicted power and predicted work over time was

determined using one- and two-factor, repeated-measures ANOVAs followed by Tukey's post hoc tests. For the one-factor ANOVA the independent variable was load (0, 1.82, 4.54, 6.36, and 9.08 kg), and the dependent variable was percent decline in maximum predicted power. The independent variables for one of the two-factor ANOVAs were load and the components of predicted power (angular velocity and torque). The dependent variable was percent decline. The independent variables for the other two-factor ANOVAs were load and contraction number (first and average of last 8). The dependent variables were predicted work, predicted excursion, and predicted torque time integral (TTI). In all cases, we considered differences to be significant at $P < 0.05$.

RESULTS

Equations for β_A , β_{K_m} , and β_{τ_1} [eqs. (4a), (7a), and (8a)] as a function of other model parameters were derived from correlations and regression analyses. The fitted β parameters were identified by minimizing the error between the measured and modeled angles and angular velocities for the 0-, 4.5-, and 9.08-kg fatiguing tests. The initial equations were derived from correlations between the fitted β parameters and both the force model parameters and the initial angular velocities and excursions. The final equations were derived from linear regression analyses, where the independent variables were both the original variables used in the correlation analysis and the initial equations derived from the correlation analysis. The dependent variables were the fitted β parameters:

$$\beta_A = \frac{-5.66 \times 10^{-3} A_{90,0,iso}^{5.5} K_{m0}^8}{\left(\max \left| \frac{d\theta}{dt} \right|_{0(12\text{Hz})}\right)^{1.3}} + 1.04 \times 10^{-5} \max \left| \frac{d\theta}{dt} \right|_{0(50\text{Hz})} - 9.13 \times 10^{-6} \max \left| \frac{d\theta}{dt} \right|_{0(12\text{Hz})} + 6.17 \times 10^{-7} \quad (4a)$$

$$\beta_{K_m} = \begin{cases} 0 & L/I > 35 \\ \frac{2.28 \times 10^{-5} \tau_{1,iso}^2}{\left(\max \theta_{0(12\text{Hz})} - \min \theta_{0(12\text{Hz})}\right)^3} - 2.11 \times 10^{-6} \left(\frac{A_{90,0,iso}}{A_{90,0}}\right)^2 + \frac{9.75 \times 10^{-5}}{F_M} - 2.70 \times 10^{-7} & L/I \leq 35 \end{cases} \quad (7a)$$

$$\beta_{\tau_1} = \begin{cases} 0 & L/I > 35 \\ 5.00 \times 10^{-6} \frac{A_{90,0,iso}^2}{\left(\max \left| \frac{d\theta}{dt} \right|_{0(12\text{Hz})}\right)^2} + 1.10 \times 10^{-1} b^2 - 1.38 \times 10^{-4} & L/I \leq 35 \end{cases} \quad (8a)$$

The subscript 0 indicates the pre-fatigue value for parameters that also have fatigue values. The subscript *iso* indicates the isometric fatigue session value; otherwise, the general non-isometric fatigue session value on the day of interest is used. The subscripts 12 Hz and 50 Hz identify the frequency used to generate that pre-fatigue contraction. We noticed that β_{K_m} and β_{τ_1} were not needed at the lowest load, 0 kg, but they were always needed at the highest load, 9.08 kg. Because L/I decreased with increasing load, we tested various values for L/I that were less than those for the 0-kg load and greater than those for the 9.08-kg load. The cut-off value was approximately $35 \text{ kg}^{-1} \text{ m}^{-1}$.

Because we were able to express β_A , β_{K_m} , β_{τ_1} as functions of pre-fatigue parameters and measurements, non-isometric fatigue measurements were no longer needed to predict non-isometric fatigue. The predicted values in all figures were obtained using the β equations. All but 5 parameters (A_{90} , K_m , τ_1 , L/I , and F_M) were identified in the isometric fatigue session. The remaining 5 parameters were identified from pre-fatigue general non-isometric measurements on the day of interest.

Both measured and predicted angular excursion decreased over time as the total number of

contractions increased; the greater the load, the greater the fatigue (Fig. 3). Predicted excursion-time curves were within 1 standard deviation of measured excursion-time curves. Statistical assessment of the predictive accuracy through linear regression analysis pointed out a limitation in comparing the different loads (Fig. 4). The results from the subject in Figure 4 clearly show that, although the r^2 for 0 kg is lower (0.56) than that for 9.08 kg (0.78), this difference was primarily due to the narrower range of values produced by 0 kg because of minimal fatigue. At loads greater than 0 kg, the average r^2 for the first (development) and second group of subjects indicates that the new force-fatigue model accounted for 70–76% and 62–69% of the variability in angular excursion, respectively (Fig. 5A). At 0 kg the model accounted for 63% and 56% of the variability, respectively. The model also accounted for 60–68% of the variability in the angular velocity (Fig. 5B). The approximate 0.13 difference in the r^2 between the 9-kg general non-isometric and the isometric fatiguing contractions suggested a small drop in accuracy when predicting non-isometric contractions ($P < 0.0305$; Fig. 5A).

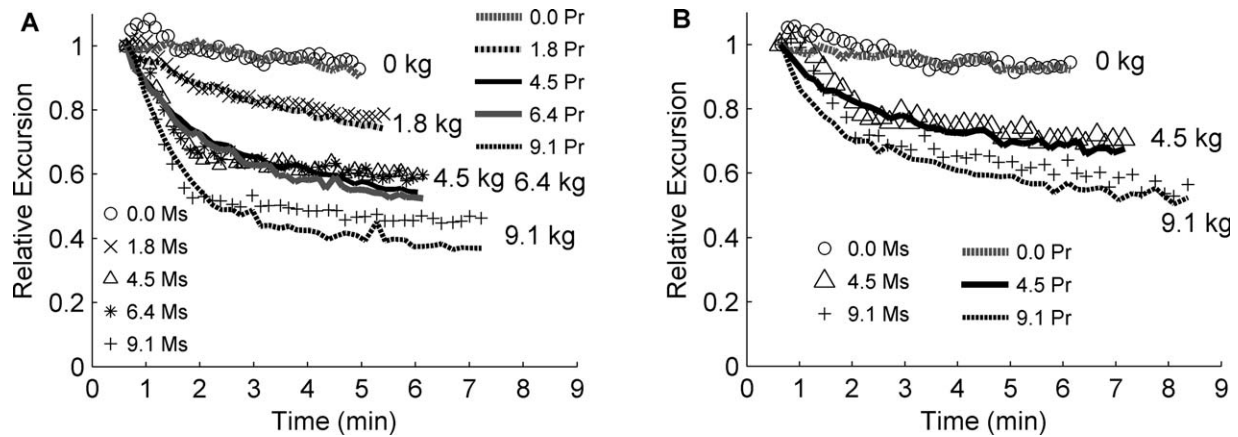


FIGURE 3. Measured (Ms) and predicted (Pr) load-dependent reduction in relative angular excursion during fatiguing contractions. Every fifth 33CFT is shown for the model development subjects (**A**) and for the model validation subjects (**B**). Contractions are normalized to the first contraction. Predicted contractions are within 1 standard deviation of the measured contractions (not shown due to congestion; i.e., standard deviations crossed adjacent means for some loads).

Although torque could not be measured directly during the general non-isometric leg extensions, it could be predicted by the model, and therefore the loss in power and work over time could be predicted. In general, the greater the load, the greater the difference between the

initial and final maximum power and total work (Figs. 6 and 7), with the 9.08-kg load showing an 84% loss in power and work. The percent decline in angular velocity at maximum power tended to be greater than the corresponding torque ($P =$

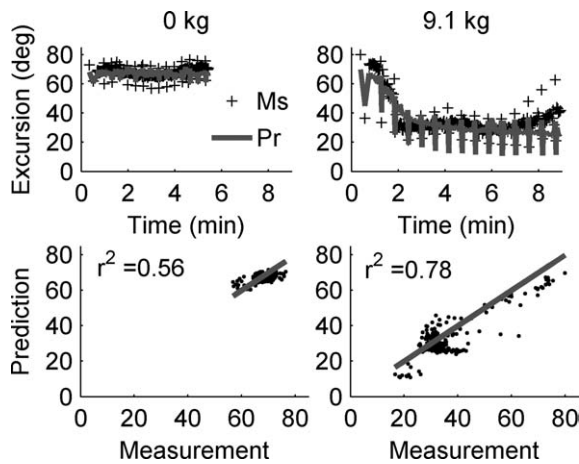


FIGURE 4. Plots of predicted (Pr) vs. measured (Ms) angular excursion from 1 subject (model development) for the 0- and 9.1-kg loads. Note that the r^2 for 9.1 kg is higher than that for 0 kg, primarily because 9.1 kg produces greater fatigue over time; that is, 9.1 kg has a wider range of values. Each pair of 50CFT and 12.5VFT testing trains was followed by 13 33CFT fatiguing trains (14 sets of 15 or a total of 210 contractions per load). Row 2 is the linear regression analysis. Both a fixed slope of unity and a y-intercept of 0 were used, because this is the ideal relationship between measurement and prediction. Initial force model parameters for the 0- and 9.1-kg loads, respectively, were: $A_{90} = 1.28$ and 1.24 N/ms; $K_m = 1.51e-01$ and $1.70e-01$; $\tau_1 = 47.8$ and 41.9 ms; $\tau_2 = 20.0$ ms, $\tau_c = 20$ ms; $R_0 = 2$; $a = -4.67e-04$ deg $^{-2}$; $b = 4.26e-02$ deg $^{-1}$; $V_1 = 5.07e-01$ N/deg 2 ; $V_2 = 2.70e-02$ deg $^{-1}$; $L/l = 67.0$ and 9.62 kg $^{-1}$ m $^{-1}$; $F_M = 60.0$ and 52.6 N. Fatigue model parameters were: $\tau_{fat} = 95.4$ s; $\alpha_A = -2.82e-07$ ms $^{-2}$; $\alpha_{Km} = -4.25e-08$ ms $^{-1}$ N $^{-1}$; $\alpha_{\tau_1} = 3.65e-05$ N $^{-1}$; $\beta_A = -3.83e-07$ and $-7.41e-10$ ms $^{-1}$ deg $^{-1}$; $\beta_{Km} = 7.81e-07$ and $3.36e-06$ deg $^{-1}$ N $^{-1}$; $\beta_{\tau_1} = 3.31e-05$ and $2.52e-04$ ms deg $^{-1}$ N $^{-1}$.

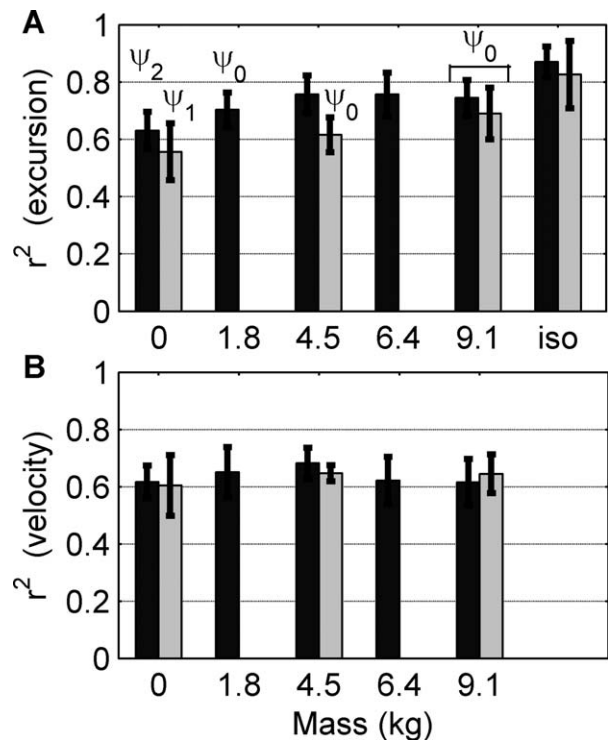


FIGURE 5. Average linear regression coefficients of determination (r^2 ; $\pm 95\%$ confidence limit; n of black bars = 9–10 subjects, n of gray bars = 7 subjects) for predicted vs. measured angular excursion (**A**) and velocity (**B**) at different loads for all contractions (50CFT, 12.5VFT, and 33CFT). Also, the r^2 for predicted vs. measured isometric torque–time integral at 90° (iso) is shown for comparison. Black bars—data from these subjects used to develop β equations; gray bars—new subjects. ψ_2 —compared with 4.5 and 6.4 kg and with isometric ($P < 0.038$); ψ_1 —compared with 9.1 kg and isometric ($P < 0.012$); ψ_0 —compared with isometric ($P < 0.031$).

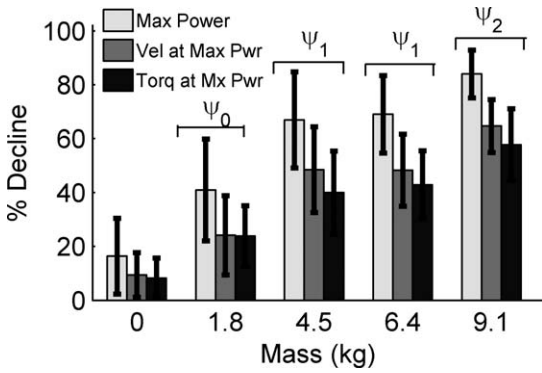


FIGURE 6. Percent decline in predicted maximum (Max) power, and predicted angular velocity (Vel) and torque (Torq) at maximum power (mean \pm SD; $n = 9$ – 10 subjects; only 33CFT). The average of the last 8 contractions was used as the final value when estimating percent decline. ψ_2 —compared with 0, 1.8, 4.5, and 6.4 kg ($P < 0.017$, note: $P = 0.068$ for max power 9.1 vs. 6.4 kg); ψ_1 —compared with 0 and 1.8 kg ($P \leq 0.006$); ψ_0 —compared with 0 kg ($P < 0.001$).

0.006); however, at any given load, the difference was not significant (Fig. 6).

DISCUSSION

The objectives of our study were to: (1) develop a model of non-isometric fatigue for electrical stimulation-induced, open-chain, repeated extensions of the leg at the knee; and (2) experimentally validate the model. The first objective was accomplished by adding angular velocity, modified by a parameter, β , to the equations for A , K_m , and τ_1 in the isometric fatigue model¹¹ [eqs. (4), (6)–(8)], so that the new equations are driven by force, such as in Ding and co-workers' isometric fatigue model,^{11,19,23} and power representing the additional fatigue generated by performance of work. The three new parameters, β_A , β_{K_m} , and β_{τ_1} , were functions of pre-fatigue parameters and pre-fatigue measurements. Non-isometric fatigue measurements were not needed to predict non-isometric fatigue. In total, all but 5 parameters (A_{90} , K_m , τ_1 , L/I , and F_M), from both the force and fatigue models, were identified from measurements collected on the day of the isometric fatigue session. The remaining 5 parameters were identified from pre-fatigue, free-swing measurements on the days of the non-isometric fatigue sessions.

Because 14 of the 19 parameters for each subject were identified in one testing session (the isometric fatigue session), and because non-isometric fatigue measurements were not needed to predict non-isometric fatigue (β_A , β_{K_m} , and β_{τ_1} equations require pre-fatigue measurements), essentially all of our free-swing fatigue measurements experimentally validated the model (the second aforementioned objective; Figs. 3 and 5). However, 10 of the subjects with loads of 0, 4.54, and 9.08 kg and one

type of fatigue stimulation protocol were used to develop the β equations. Therefore, the results for loads 1.82 and 6.36 kg from those same 10 subjects and the results for loads of 0, 4.54, and 9.08 kg from 7 new subjects using a different type of fatigue stimulation protocol better demonstrated the predictive accuracy of the model (Figs. 3 and 5). The new force-fatigue model accounted for at least 60% of the variability in the angle and angular velocity during the free-swing fatiguing leg extensions (Fig. 5).

The predictive ability of our new non-isometric force-fatigue model is not as high as that of our isometric force-fatigue model. Because there is no experimentally validated model in the literature that can predict non-isometric fatigue in humans, we compared our non-isometric predictions to our isometric predictions. The isometric force-fatigue model used in this study accounted for 83–87% of the variability in the TTI when fit to the measurements (Fig. 5A) and at least 75% of the variability in the TTI when predicting the measurements from our recently published study on the effect of muscle length on fatigue.¹⁹ Although the non-isometric force-fatigue model accounted for more than 60% of the variability in the TTI when

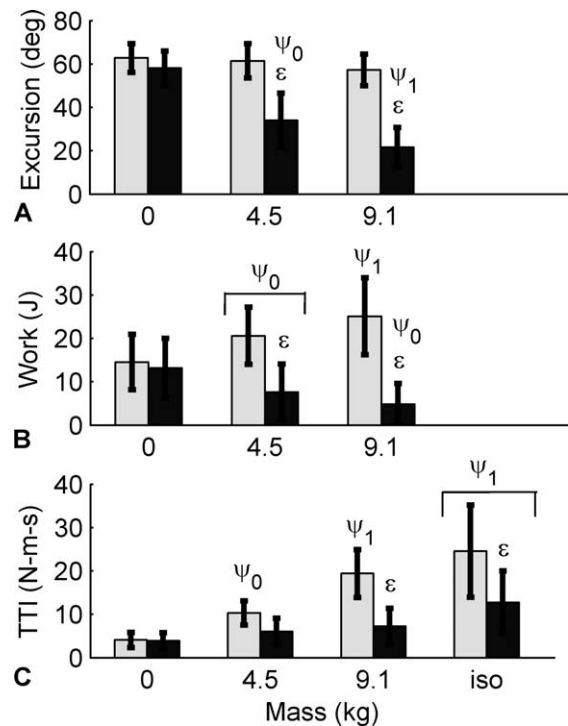


FIGURE 7. Predicted excursion (A), work (B), and torque time integral (TTI) (C) (mean \pm SD; $n = 10$ subjects; 33CFT). Isometric torque time integral (iso) is shown for comparison. Gray bars—first contraction; black bars—average of last 8 contractions. ϵ —compared with first contraction ($P < 0.0001$); ψ_1 —compared with 0 and 4.5 kg ($P \leq 0.037$); ψ_0 —compared with 0 kg ($P \leq 0.018$).

predicting the measurements, this was about 15% less than that accounted for by the isometric force–fatigue model. Several factors may account for the 15% difference between the r^2 values for the isometric and non-isometric fatigue predictions:

1. Although electrodes were positioned such that the torque–time curves were nearly textbook at three isometric knee angles, the number and types of muscle fibers recruited during each leg extension and from day-to-day during the non-isometric fatigue sessions may not have been as consistent as they were for the isometric session. This is because the leg was free to move, allowing for greater movement of the quadriceps muscles relative to the electrodes.
2. During isometric leg extensions, the leg remained in the sagittal plane. During free-swinging leg extensions the leg may have moved out of the sagittal plane, especially as it fatigued, even though electrode placement attempted to minimize non-extension movements.
3. We manually stopped and released the leg after each fatiguing extension by using our hands. Sometimes the stop and resting positions were not identical and, occasionally, we released immediately after the next train started, rather than beforehand. This would have altered the velocity of that leg extension.
4. Although the muscles were potentiated just prior to every test to minimize this confounding factor, additional potentiation still occurred at the beginning of the fatigue protocol, especially at the lowest loads (Fig. 3). We could not eliminate this additional potentiation completely and still use the same protocol for all loads without initiating fatigue at the highest loads.

Our experimental results are similar to those of Lee and co-workers, who investigated the effects of load on fatigue during electrically stimulated leg extensions in humans.²⁷ Both the percent decline in excursion and the initial work performed at the low loads (Figs. 5A, 6, and 7B)²⁷ in their study were comparable to our results (Figs. 3A and 7A, B). The percent decline in power and work in their study were different from our results for at least two reasons. First, their fatiguing trains were 40CFT, 0.15 second in duration. Our fatiguing trains were 33CFT, approximately 0.15–1 second in duration, depending on the load applied and on the subject. Our train duration was set to produce a constant initial excursion at all loads (Fig. 7A), whereas their initial excursion decreased with increasing load (Fig. 7A in their investigation). Our goal was to generate as much fatigue as possi-

ble at each load without changing the stimulation frequency, amplitude, or pulse duration. Therefore, we used as large a range in excursion as possible between the initial pre-fatigue value and the final fatigue value to help develop a fatigue model that could easily differentiate between several different loads. As a result, the difference in fatigue between the loads in our study was a result of both the load itself and the train duty cycle, such that the highest load had the highest train duty cycle and the greatest fatigue. A second reason for the differences in percent decline in power and work between our two studies is that they used a dynamometer, set in the isotonic mode, to mimic the application of a constant load, and to record knee angles. We applied weights and attached an electrogoniometer to a free-moving leg. The response time of the dynamometer is likely slower than that of the leg. The electrogoniometer detects changes in the knee angle even when this change does not affect the position of the dynamometer arm.

Our new non-isometric force–fatigue model could be useful to scientists researching the etiology of non-isometric peripheral fatigue at the muscle level.^{2–5} Our model can predict force in testing situations where force cannot be measured easily, such as during general non-isometric leg extensions (Figs. 6 and 7). This would allow investigators to predict losses in both force and velocity (Fig. 6) during various testing conditions. Power is determined not only by the number and force of the strongly bound cross-bridges but also by the rate of cross-bridge cycling.¹ Because fatigue is task-dependent,²⁸ quantitative comparisons between the relative loss of isometric force, non-isometric force, and velocity would help decipher the etiology of non-isometric fatigue.^{2–5}

The non-isometric force–fatigue model also could be useful to scientists and engineers who are working to improve the task performance of FES systems.^{29–32} The non-isometric force model was used in a previous study³² to predict a unique stimulation pattern for each subject to achieve the desired trajectory. The stimulation pattern chosen initially, prior to fatigue, may become less ideal as the muscle fatigues, no longer allowing the subject to achieve the same trajectory.³⁰ Therefore, the non-isometric fatigue model must be used in conjunction with the non-isometric force model to continually predict new stimulation patterns over time so that the subject can achieve the desired trajectory repeatedly. Because this non-isometric force–fatigue model will be able to generate subject- and task-specific stimulation patterns that will maintain a desired force and motion for a desired length of time, it has the potential for use as a feed-forward model in FES systems.³³ If a system

either does not use a feed-forward model or requires faster real-time output, then this model could be used to test the performance of the system prior to patient use. The model could generate a series of task-specific optimal stimulation patterns, and these patterns could be compared with the real-time FES system selections to optimize the system.

The clinical significance of our non-isometric force-fatigue model cannot be determined until further work is done on paralyzed subjects, in whom fatigue resistance will be affected by the extent of muscle atrophy³⁴ and fiber-type transformation,³⁵ which can vary considerably from person to person.³⁶ The isometric force model has been shown to perform equally well for both able-bodied and SCI-injured subjects. It required only minor modifications of the procedure used to identify the parameter values.^{37,38} The non-isometric force-fatigue model may be equally robust. It may require only minor modifications, but this remains to be demonstrated.

Because able-bodied subjects were tested in our study, there is a small chance that volitional contractions occurred during stimulation. However, it is unlikely that volitional contractions, if present, substantively affected our results. The force-fatigue model has been shown to successfully predict fatigue in response to different frequencies and pulse patterns for numerous subjects over many years.^{11,21,23,38,39} This indicates that the signal-to-noise ratio has been high, where here the stimulated contractions corresponded to the signal and the volitional contractions corresponded to the noise. In all cases, several testing sessions were performed on each subject, and each session was separated by 48 hours.

Two existing mathematical models, one of non-isometric force and the other of isometric fatigue, were used to develop the non-isometric force-fatigue model. Angular velocity and three new parameters (β_A , β_{Kmv} , and $\beta_{\tau 1}$) were added to the isometric fatigue model to account for power produced during the contractions. The new fatigue model parameters were solely functions of the force model parameters, and therefore measurements of non-isometric fatigue are not needed to predict non-isometric fatigue. More than 60% of the variability in the measurements was explained by the new force-fatigue model. This new non-isometric force-fatigue model can be used by scientists to research the etiology of non-isometric fatigue and by scientists and engineers to improve the task performance of FES systems.

This work was supported in part by a grant from the National Institute for Disability Related Research (NIDRR, Award No.

H133G0200137). The authors thank the California Alliance for Minority Participation (CAMP) students, Cheryl-Lynn Chow and Carmen Valladares, for their technical assistance.

REFERENCES

1. Fitts RH. The cross-bridge cycle and skeletal muscle fatigue. *J Appl Physiol* 2008;104:551–558.
2. Ameredes BT, Brechue WF, Andrew GM, Stainsby WN. Force-velocity shifts with repetitive isometric and isotonic contractions of canine gastrocnemius in situ. *J Appl Physiol* 1992;73:2105–2111.
3. Cheng AJ, Rice CL. Fatigue and recovery of power and isometric torque following isotonic knee extensions. *J Appl Physiol* 2005;99:1446–1452.
4. James C, Sacco P, Jones DA. Loss of power during fatigue of human leg muscles. *J Physiol* 1995;484:237–246.
5. Jones DA, de Ruyter CJ, de Haan A. Change in contractile properties of human muscle in relationship to the loss of power and slowing of relaxation seen with fatigue. *J Physiol* 2006;576:913–922.
6. Cairns SP, Knicker AJ, Thompson MW, Sjogaard G. Evaluation of models used to study neuromuscular fatigue. *Exerc Sport Sci Rev* 2005;33:9–16.
7. Ferrarin M, Pedotti A. The relationship between electrical stimulus and joint torque: a dynamic model. *IEEE Trans Rehabil Eng* 2000;8:342–352.
8. Perumal R, Wexler AS, Binder-Macleod SA. Mathematical model that predicts lower leg motion in response to electrical stimulation. *J Biomech* 2006;39:2826–2836.
9. Perumal R, Wexler AS, Binder-Macleod SA. Development of a mathematical model for predicting electrically elicited quadriceps femoris muscle forces during isovelocity knee joint motion. *J Neuroeng Rehabil* 2008;5:33.
10. Shorten PR, O'Callaghan P, Davidson JB, Soboleva TK. A mathematical model of fatigue in skeletal muscle force contraction. *J Muscle Res Cell Motil* 2007;28:293–313.
11. Ding J, Wexler AS, Binder-Macleod SA. Mathematical models for fatigue minimization during functional electrical stimulation. *J Electromyogr Kinesiol* 2003;13:575–588.
12. Giat Y, Mizrahi J, Levy M. A musculotendon model of the fatigue profiles of paralyzed quadriceps muscle under FES. *IEEE Trans Biomed Eng* 1993;40:664–674.
13. Rienen R, Quintern J, Schmidt G. Biomechanical model of the human knee evaluated by neuromuscular stimulation. *J Biomech* 1996;29:1157–1167.
14. Hawkins D, Hull ML. Muscle force as affected by fatigue: mathematical model and experimental verification. *J Biomech* 1993;26:1117–1128.
15. Tang CY, Stojanovic B, Tsui CP, Kojic M. Modeling of muscle fatigue using Hill's model. *Biomed Mater Eng* 2005;15:341–348.
16. Xia T, Frey Law LA. A theoretical approach for modeling peripheral muscle fatigue and recovery. *J Biomech* 2008;41:3046–3052.
17. Ma L, Chablat D, Bennis F, Zhang W. A new simple dynamic muscle fatigue model and its validation. *Int J Indust Ergonom* 2009;39:211–220.
18. Wexler AS, Ding J, Binder-Macleod SA. A mathematical model that predicts skeletal muscle force. *IEEE Trans Biomed Eng* 1997;44:337–348.
19. Marion MS, Wexler AS, Hull ML, Binder-Macleod SA. Predicting the effect of muscle length on fatigue during electrical stimulation. *Muscle Nerve* 2009;40:573–581.
20. Perumal R, Wexler AS, Ding J, Binder-Macleod SA. Modeling the length dependence of isometric force in human quadriceps muscles. *J Biomech* 2002;35:919–930.
21. Ding J, Wexler AS, Binder-Macleod SA. A predictive model of fatigue in human skeletal muscles. *J Appl Physiol* 2000;89:1322–1332.
22. Merton PA. Voluntary strength and fatigue. *J Physiol* 1954;123:553–564.
23. Ding J, Wexler AS, Binder-Macleod SA. A predictive fatigue model—I: Predicting the effect of stimulation frequency and pattern on fatigue. *IEEE Trans Neural Syst Rehabil Eng* 2002;10:48–58.
24. Birge B. PSOt—a particle swarm optimization toolbox for use with MatLab. Indianapolis, IN: IEEE; 2003. p 182–186.
25. Ding J, Wexler AS, Binder-Macleod SA. A predictive fatigue model—II: Predicting the effect of resting times on fatigue. *IEEE Trans Neural Syst Rehabil Eng* 2002;10:59–67.
26. Coleman TF, Li YY. An interior trust region approach for nonlinear minimization subject to bounds. *SIAM J Optimization* 1996;6:418–445.
27. Lee SC, Becker CN, Binder-Macleod SA. Activation of human quadriceps femoris muscle during dynamic contractions: effects of load on fatigue. *J Appl Physiol* 2000;89:926–936.
28. Maluf KS, Enoka RM. Task failure during fatiguing contractions performed by humans. *J Appl Physiol* 2005;99:389–396.

29. Chou LW, Kesar TM, Binder-Macleod SA. Using customized rate-coding and recruitment strategies to maintain forces during repetitive activation of human muscles. *Phys Ther* 2008;88:363–375.
30. Kebaetse MB, Turner AE, Binder-Macleod SA. Effects of stimulation frequencies and patterns on performance of repetitive, nonisometric tasks. *J Appl Physiol* 2002;92:109–116.
31. Kesar T, Chou LW, Binder-Macleod SA. Effects of stimulation frequency versus pulse duration modulation on muscle fatigue. *J Electromyogr Kinesiol* 2008;18:662–671.
32. Maladen RD, Perumal R, Wexler AS, Binder-Macleod SA. Effects of activation pattern on nonisometric human skeletal muscle performance. *J Appl Physiol* 2007;102:1985–1991.
33. Bobet J. Can muscle models improve FES-assisted walking after spinal cord injury? *J Electromyogr Kinesiol* 1998;8:125–132.
34. Castro MJ, Apple DF Jr, Staron RS, Campos GE, Dudley GA. Influence of complete spinal cord injury on skeletal muscle within 6 mo of injury. *J Appl Physiol* 1999;86:350–358.
35. Burnham R, Martin T, Stein R, Bell G, MacLean I, Steadward R. Skeletal muscle fibre type transformation following spinal cord injury. *Spinal Cord* 1997;35:86–91.
36. Gerrits HL, Hopman MT, Offringa C, Van Engelen BG, Sargeant AJ, Jones DA, et al. Variability in fibre properties in paralysed human quadriceps muscles and effects of training. *Pflugers Arch* 2003;445:734–740.
37. Ding J, Chou LW, Kesar TM, Lee SC, Johnston TE, Wexler AS, et al. Mathematical model that predicts the force–intensity and force–frequency relationships after spinal cord injuries. *Muscle Nerve* 2007;36:214–222.
38. Ding J, Lee SC, Johnston TE, Wexler AS, Scott WB, Binder-Macleod SA. Mathematical model that predicts isometric muscle forces for individuals with spinal cord injuries. *Muscle Nerve* 2005;31:702–712.
39. Chou LW, Ding J, Wexler AS, Binder-Macleod SA. Predicting optimal electrical stimulation for repetitive human muscle activation. *J Electromyogr Kinesiol* 2005;15:300–309.